

Hong Kong  
Environmental Protection  
Department

---

**Agreement No.  
CE57/2006 (EP) Review  
of Air Objectives and  
Development of a Long  
Term Air Quality  
Strategy for Hong Kong  
- Feasibility Study**

---

Appendix I

Modelling Results

ARUP



# I1 Prediction of Air Quality Upon Implementation of Proposed Control Measures

## I1.1 The PATH Model

The Pollutants in the Atmosphere and their Transport over Hong Kong (PATH) model is used for projecting the air quality in the future years in this Study. Following provides an overview of this model and its features.

The PATH model consists of 3 core modules:

- **EMS-95** for Emission Inventory
- **MM5** for Conditioning for Meteorology, Terrain, Landuse;
- **SAQM** (Multi-species photochemical air quality model) for Pollutants Transport & Chemistry Modelling

### I1.1.1 EMS-95

The EMS-95 processes emission for point, area based, motor vehicle, and biogenic sources from raw data. The sub-modules summarized in **Table I1.1** are used to determine the emission through the EMS-95 modules.

**Table I1.1:** Functions of the EMS-95 sub-modulus

Modulus	Functions	Remarks
Point Source Model	Processes source emissions for which exact location and properties are known.	<ul style="list-style-type: none"> <li>• Power Plant Emission</li> <li>• Industrial Emission</li> <li>• Quarries (HK)</li> </ul>
Area Source Model	Processes the source emissions of county-wide sources into hourly emissions of grid cell based sources.	<ul style="list-style-type: none"> <li>• Marine Emission</li> <li>• Transportation Emission</li> <li>• Rail Emission</li> <li>• Quarries Emission (PRD)</li> <li>• Airport Emission</li> </ul>
Biogenics Model	Generates biogenic emission from raw data	<ul style="list-style-type: none"> <li>• VOC emission from different land use</li> </ul>
Grid Definition Model	Generates modelling grid using GIS for defining the spatial distribution of the sources	<ul style="list-style-type: none"> <li>•</li> </ul>
Speciation Model	Computes the lumped aggregated emissions into chemical species suitable for simulation.	<ul style="list-style-type: none"> <li>•</li> </ul>

### I1.1.2 MM5

MM5 provides a multi-scale non-hydrostatic model with parameterised cloud microphysics for simulation of boundary layer turbulence. It is used to generate 3D fields of wind, turbulence, temperature, humidity and cloud convection. These data sets are input through process filter for the air quality model SAQM to simulate transport diffusion and chemical reactions of various pollutants. Yr 2003 MM5 data was provided by EPD for the assessment in this study.

### I1.1.3 SAQM

The SAQM model made use of the complex 3D air chemistry models to resolve a set of mass balance equations on a grid for a number of non-reactive and reactive species. In addition to the mass conservation approach to dispersion, SAQM also resolves a set of chemical species conversion equations to determine the pollutant concentration. The concentration and wind are decomposed into their mean and variance component, and

Reynolds averaging is applied. It is a derivative of the much-used and tested Regional Acid Deposition Model (RADM). The SAQM model runs on a series of nests with grid spacing ranging from 40.5km down to 0.5km. The current assessment adopts a 1.5km grid resolution. There are two major sources of changes for a species in SAQM: transportation and chemistry. Emissions into appropriate grid cells are lumped with the deposition (the lowest layer only) and the production and destruction rates simulated for each species before integration. The conservation equations consist of the mean concentrations and the flux terms resulting from changes in the mean concentration. The emissions and gas phase chemistry process are interlaced between the physical processes for each advection time step. The model resolves the physical processes for half an advection step, resolves the emission /gas-phase chemistry and aerosol chemistry for an entire advection step, and then resolves the physical processes in the reverse order for the remaining half advection step. SAQM carries these computations for a total of 37 chemical species.

Species transport in SAQM utilises the meteorological fields from MM5. In particular, three dimensional wind and temperature data are used in the transport calculations. Additional fields, such as surface-layer parameters, are also needed to account for the sub-grid scale turbulent transport. In SAQM, the numerical advection scheme uses locally fitted polynomials of arbitrary order to compute the flux between adjacent grid cells and then applies a flux limitation step to assure a positive definition solution.

Two turbulent mixing schemes are available in SAQM:

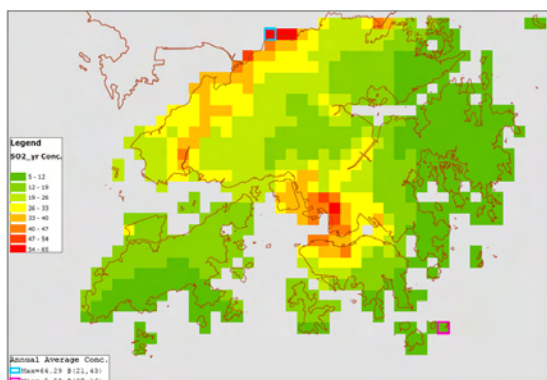
- Non-local K approach based on a representation of the K profile in a well mixed Planetary Boundary Layer (PBL); and
- A transient turbulent representation, which allows a range of eddy sizes to contribute to the turbulent mixing process. Vertical mixing is represented in flux form and the non-local turbulent closure algorithm used is the Asymmetric Convection Model (ACM), which employs different mixing schemes in the updraft and downdraft sections of the convective boundary layer.

Chemistry process mechanism in SAQM makes use of the Carbon Bond-IV (CB-IV). This approach lumps organic species according to bond type (e.g. single carbon bonds, double carbon bonds, carbonyl bonds). This structured lumping technique categorises the reactions of similar carbon bonds and is opposed to the molecular lumping approach that groups the reactions of entire molecules.

In order to accommodate particulate matter in PATH, 6 additional chemical species have been added to the 29 species originally handled by SAQM. They are gas phase NH<sub>3</sub>, hydrogen ion concentration and aerosol phase sulphate, nitrate, ammonia and water. Similarly, since the SAQM CBM4 mechanism did not calculate gas phase NH<sub>3</sub> concentration, 6 additional reactions were included in the 83 reactions adopted in CB-IV.

The Photochemical smog precursors, Primary Particulate precursors and Particulate precursors are used to model the CO, PM<sub>10</sub>, SO<sub>2</sub>, NO<sub>x</sub> and VOC.

Results from the SAQM of PATH model are extracted in the form of hourly pollutant levels. Pollutant concentrations are established in 1.5km x 1.5 km grids cell with vertical levels ranging from 0 to 24,232m. **Figure I1.1** shows a sample spatial distribution of the predicted concentrations.

**Figure I1.1:** Sample analyses outputs: The spatial distribution of concentration

## I1.2 Proposed New Measures Scenarios

### I1.2.1 Assessment Scenarios

Assessments are made corresponding to the following scenarios:

- Phase I control measures
- Phase II control measures
- Phase III control measures

Assumptions and emission levels for above scenarios have been summarized in **Appendix G**.

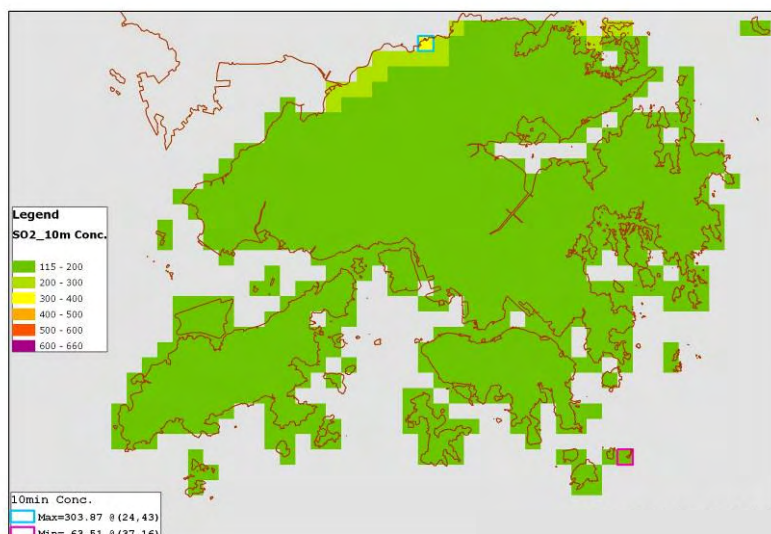
### I1.2.2 Phase I Control Measures

#### I1.2.2.1 Sulphur Dioxide

PATH model run has been conducted on SO<sub>2</sub>. As the PATH model does not have the algorithm for predicting concentrations with averaging time less than 1 hour, the 10min SO<sub>2</sub> concentrations are derived from the respective predicted 1-hr SO<sub>2</sub> levels. Based on the monitoring data in Yr 2003, the ratios of max 10-min SO<sub>2</sub> to max 1-hr SO<sub>2</sub> are found ranging from 1.06 (Tap Mun) to 1.70 (Tung Chung). The average ratio of 10-min SO<sub>2</sub> to 1-hr SO<sub>2</sub> of 1.28 has thus been adopted in this study.

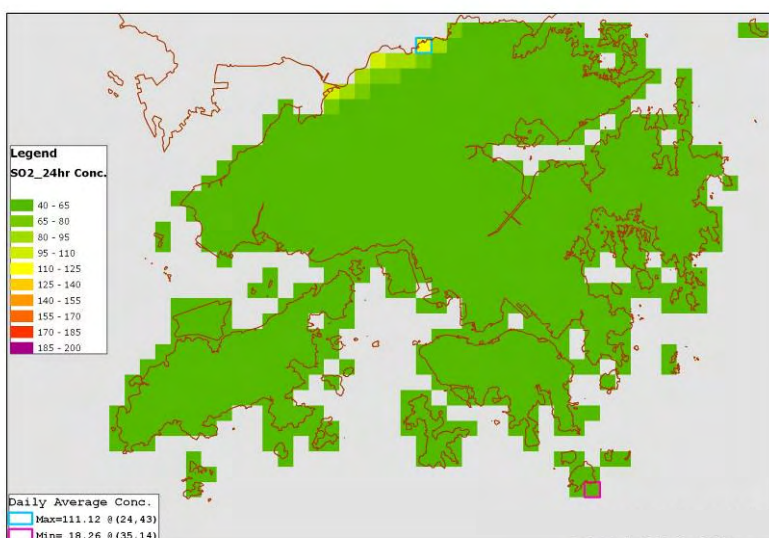
The spatial distribution of the 4<sup>th</sup> highest 10-min SO<sub>2</sub> is shown in **Figure I1.2**. The highest figure upon the implementation of Phase I control measures is 304 µg/m<sup>3</sup>, which is in compliance with the respective proposed new AQO of 500 µg/m<sup>3</sup>.

**Figure I1.2:** Spatial distribution of 4<sup>th</sup> highest 10-min SO<sub>2</sub> concentration upon implementation of Phase I measures



The spatial distribution of the 4<sup>th</sup> highest 24-hr averaged SO<sub>2</sub> is shown in **Figure I1.3**. The highest figure upon the implementation of Phase I control measures is 111 µg/m<sup>3</sup> which is in compliance with the respective proposed new AQO of 125 µg/m<sup>3</sup>.

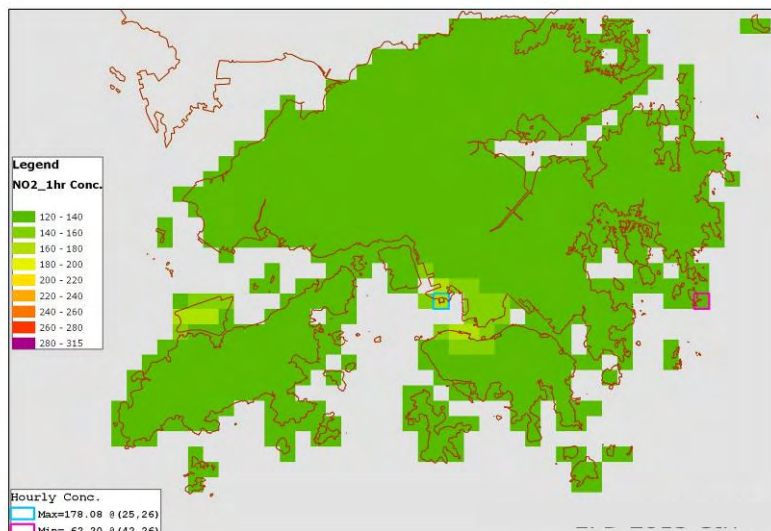
**Figure I1.3:** Spatial distribution of 4<sup>th</sup> highest 24-hr averaged SO<sub>2</sub> concentration upon implementation of Phase I measures



#### I1.2.2.2 Nitrogen Dioxide

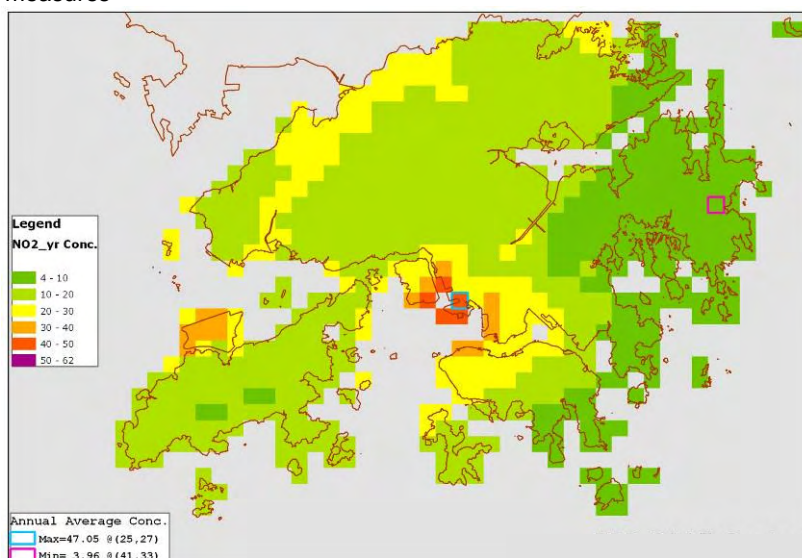
PATH model run has been conducted on 1-hr NO<sub>2</sub>. The spatial distribution of the 19<sup>th</sup> highest 1-hr NO<sub>2</sub> concentrations is shown in **Figure I1.4**. The highest figure upon the implementation of Phase I control measures is 178 µg/m<sup>3</sup>, which is in compliance with the respective proposed new AQO of 200 µg/m<sup>3</sup>.

**Figure I1.4:** Spatial distribution of 19<sup>th</sup> highest 1-hr NO<sub>2</sub> concentration upon implementation of Phase I measures



The spatial distribution of the annual NO<sub>2</sub> concentrations is shown in **Figure I1.5**. Other than a few spots at the container terminal areas which are of less concern to the general public, all general ambient locations are in compliance with the respective proposed new AQO. Similar to practice of other countries such as UK, long term (i.e., annual) AQO will not be applicable to places of work where members of the public do not have regular access. The highest figure at other locations is 39.9 $\mu$ g/m<sup>3</sup>, which is less than the respective proposed new AQO value of 40 $\mu$ g/m<sup>3</sup>.

**Figure I1.5:** Spatial distribution of annual NO<sub>2</sub> concentration upon implementation of Phase I measures

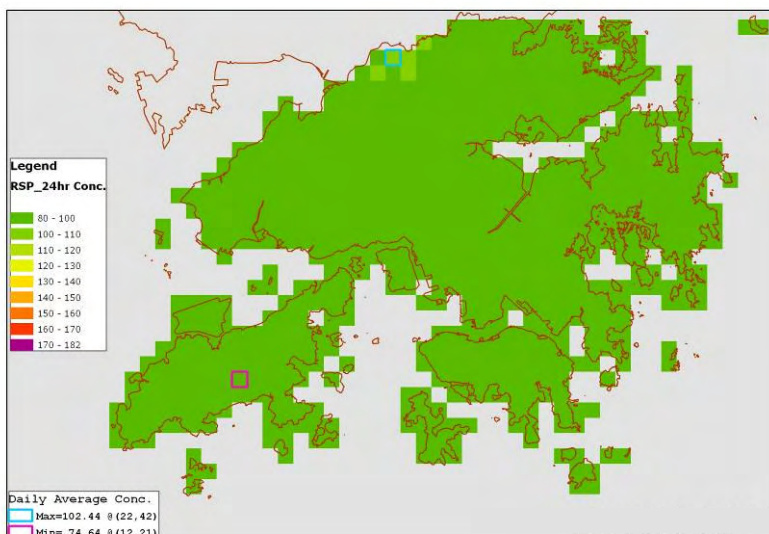


### I1.2.2.3 Respirable Suspended Particulates (PM<sub>10</sub>)

PATH model run has been conducted on 24-hr averaged and annual PM<sub>10</sub>. The spatial distribution of the 10<sup>th</sup> highest 24-hr averaged PM<sub>10</sub> concentration is shown in **Figure I1.6**. The highest figure upon implementation of the Phase I control measures is 102  $\mu$ g/m<sup>3</sup>, which is marginally higher than the respective proposed new AQO of 100  $\mu$ g/m<sup>3</sup>. Owing to the susceptibility of being influenced by trans-boundary air pollution, the maximum 24-hr averaged PM<sub>10</sub> concentration would be observed at the boundary with Shenzhen. Other than the few spots at the area near the boundary, the highest figure is 100  $\mu$ g/m<sup>3</sup>, which is in compliance with the respective proposed new AQO.

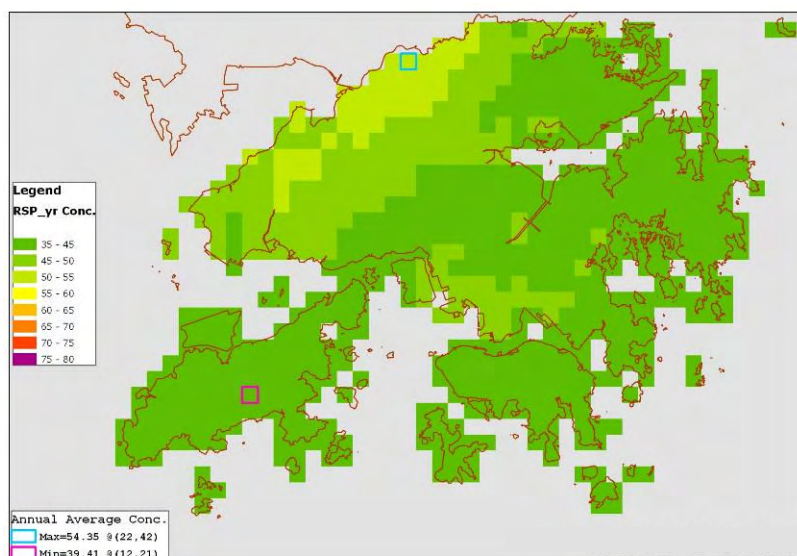


**Figure I1.6:** Spatial distribution of 10<sup>th</sup> highest 24-hr averaged PM<sub>10</sub> concentration upon implementation of Phase I measures



Similar to the 24-hr averaged PM<sub>10</sub> concentration, the highest annual PM<sub>10</sub> concentration would be observed at the boundary with Shenzhen. The predicted concentration is 54  $\mu\text{g}/\text{m}^3$ , which is marginally higher than the respective proposed new AQO of 50  $\mu\text{g}/\text{m}^3$ . The spatial distribution of the annual averaged PM<sub>10</sub> concentrations is shown in **Figure I1.7**.

**Figure I1.7:** Spatial distribution of annual PM<sub>10</sub> concentration upon implementation of Phase I measures

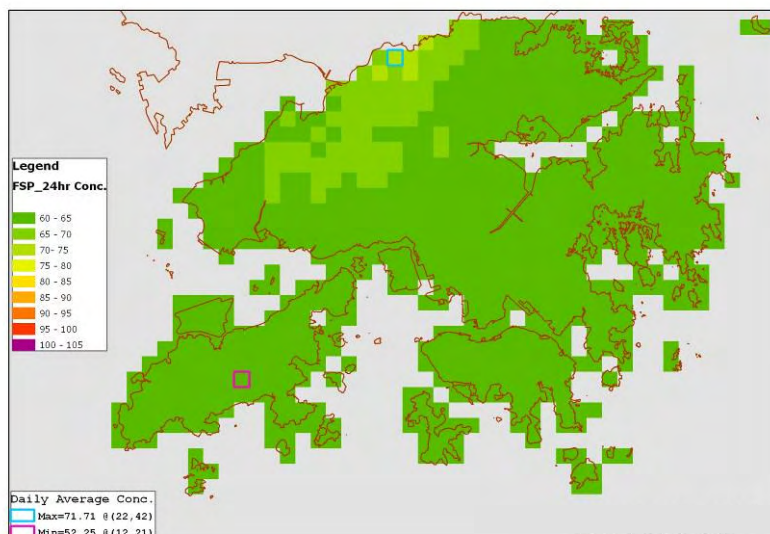


#### I1.2.2.4 Fine Suspended Particulates (PM<sub>2.5</sub>)

The PM<sub>2.5</sub> levels were estimated by multiplying the average PM<sub>2.5</sub>/PM<sub>10</sub> ratio of 0.7 (derived from existing air quality monitoring stations) on the predicted PM<sub>10</sub> value. The spatial distribution of the 10<sup>th</sup> highest 24-hr averaged PM<sub>2.5</sub> concentration is shown in **Figure I1.8**. The highest figure upon implementation of Phase I control measures is estimated to be about 72  $\mu\text{g}/\text{m}^3$ , which is in compliance with the respective proposed new AQO value of 75  $\mu\text{g}/\text{m}^3$ .

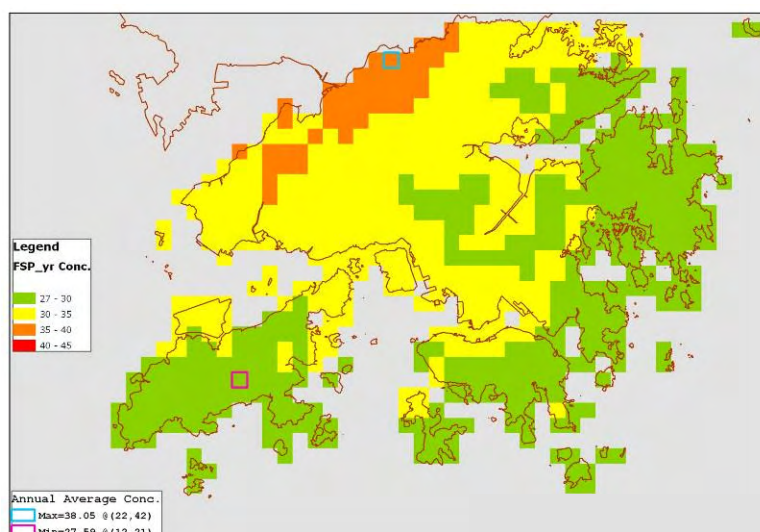


**Figure I1.8:** Spatial distribution of the 10<sup>th</sup> highest 24-hr averaged PM<sub>2.5</sub> concentration upon implementation of Phase I measures



Similar to PM<sub>10</sub>, the highest annual PM<sub>2.5</sub> concentration would be expected to occur at the boundary with Shenzhen. Due to the likely contribution of the trans-boundary emissions, the annual PM<sub>2.5</sub> concentration, upon implementation of Phase I control measures, would be 38 µg/m<sup>3</sup>, which is marginally higher than the respective proposed new AQO value of 35 µg/m<sup>3</sup>. The spatial distribution of the annual averaged PM<sub>2.5</sub> concentrations are shown in **Figure I1.9**.

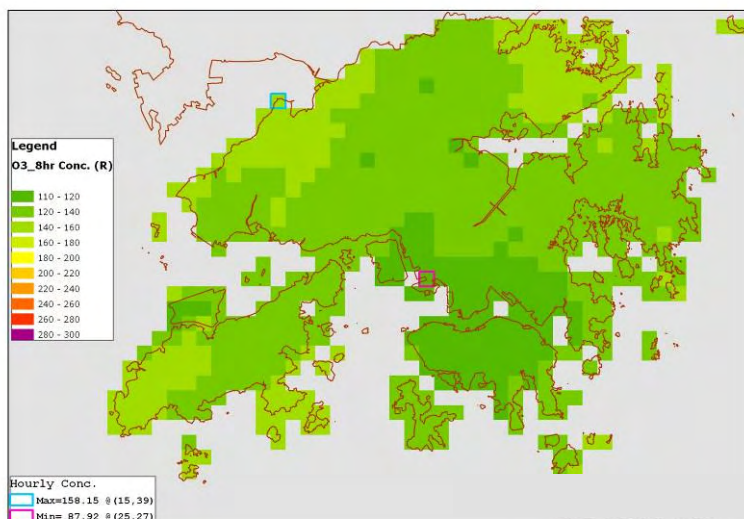
**Figure I1.9:** Spatial distribution of annual PM<sub>2.5</sub> concentration upon implementation of Phase I measures



#### I1.2.2.5 Ozone

PATH model run has been conducted for ozone. The spatial distribution of the 10<sup>th</sup> highest 8-hr averaged ozone concentrations is shown in **Figure I1.10**. The highest figure upon implementation of Phase I measures is 158 µg/m<sup>3</sup>, which is in compliance with the respective proposed new AQO.

**Figure I1.10:** Spatial distribution of 10<sup>th</sup> highest 8-hr averaged Ozone concentration upon implementation of Phase I measures



#### I1.2.2.6 Carbon Monoxide and Lead

PATH model run has not been conducted for carbon monoxide and lead as they have already been in compliance with the respective proposed new AQOs. It is expected that the compliance status will be maintained as the emissions would further be reduced upon the implementation of Phase I control measures.

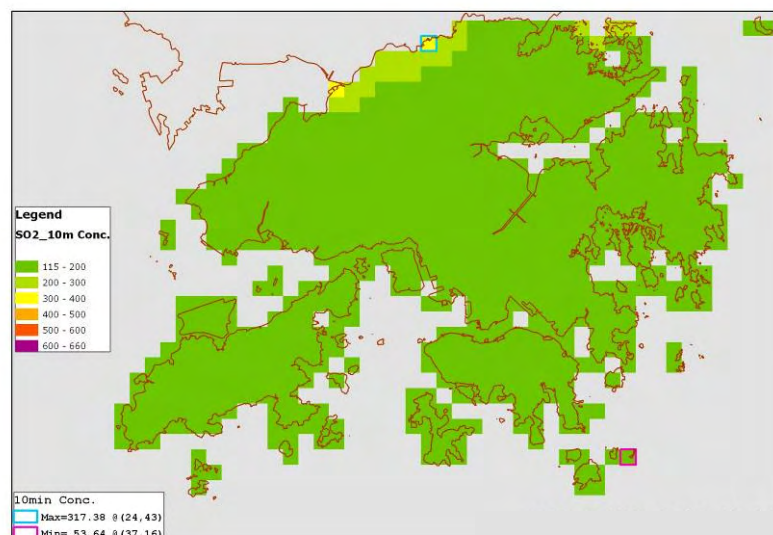
### I1.2.3 Phase II Control Measures

#### I1.2.3.1 Sulphur Dioxide

PATH model run has been conducted on SO<sub>2</sub>. As the PATH model does not have the algorithm for predicting concentrations with averaging time less than 1 hour, the 10min SO<sub>2</sub> concentrations are derived from the respective predicted 1-hr SO<sub>2</sub> levels. In order to determine the 10-min SO<sub>2</sub>, empirical relationship has been established (Please refer to section H1.2.2.1 for the relationship).

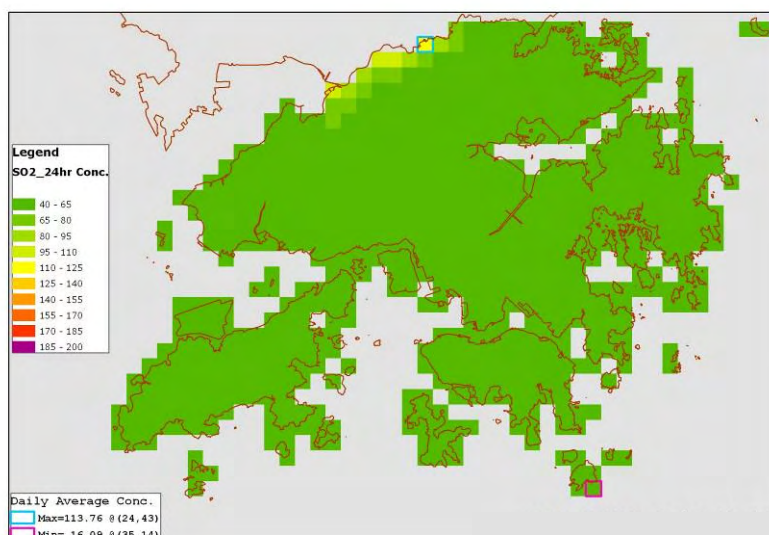
The spatial distribution of 4<sup>th</sup> highest 10-min SO<sub>2</sub> is shown in **Figure I1.11**. The highest figure upon the implementation of Phase II control measures is 317 µg/m<sup>3</sup>, which is in compliance with the respective proposed new AQO of 500 µg/m<sup>3</sup>.

**Figure I1.11:** Spatial distribution of 4<sup>th</sup> highest 10-min SO<sub>2</sub> concentration upon implementation of Phase II measures



The spatial distribution of 4<sup>th</sup> highest 24-hr averaged SO<sub>2</sub> is shown in **Figure I1.12**. The highest figure upon the implementation of Phase II control measures is 114 µg/m<sup>3</sup> which is in compliance with the respective proposed new AQO of 125 µg/m<sup>3</sup>.

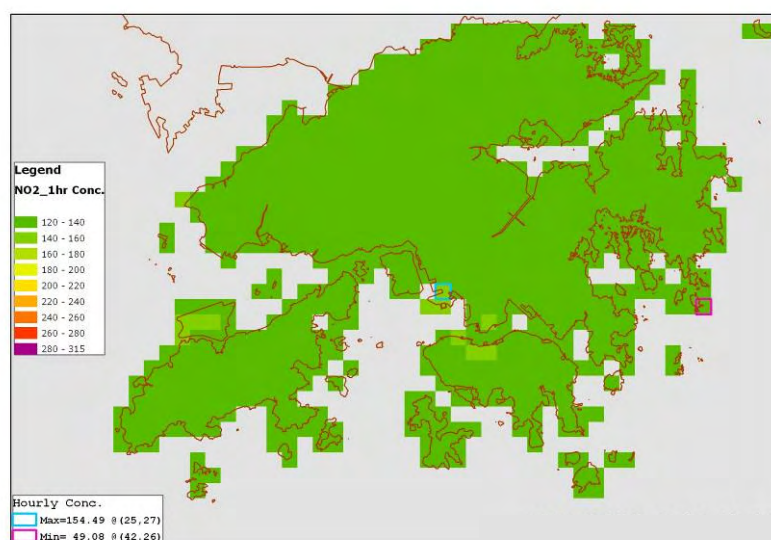
**Figure I1.12:** Spatial distribution of 4<sup>th</sup> highest 24-hr averaged SO<sub>2</sub> concentration upon implementation of Phase II measures



### I1.2.3.2 Nitrogen Dioxide

PATH model run has been conducted on 1-hr NO<sub>2</sub>. The spatial distribution of the 19<sup>th</sup> highest 1-hr NO<sub>2</sub> concentrations is shown in **Figure I1.13**. The highest figure upon the implementation of Phase II control measures is 154 µg/m<sup>3</sup>, which is in compliance with the respective proposed new AQO of 200 µg/m<sup>3</sup>.

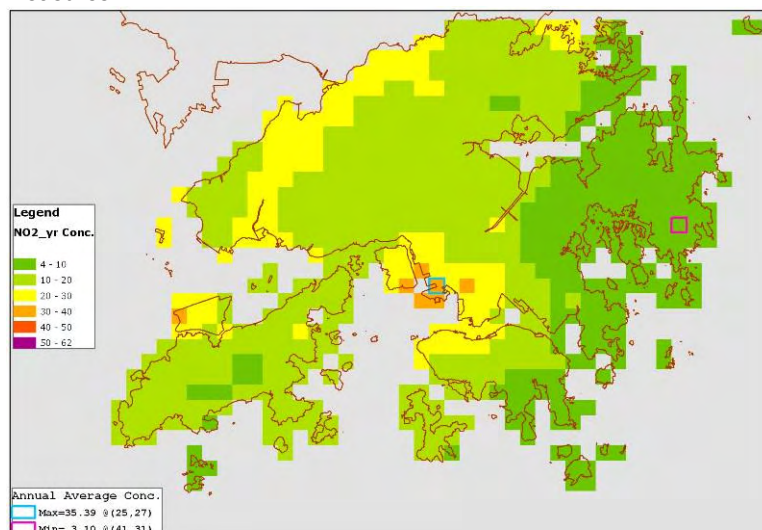
**Figure I1.13:** Spatial distribution of 19<sup>th</sup> highest 1-hr NO<sub>2</sub> concentration upon implementation of Phase II measures



The spatial distribution of the annual NO<sub>2</sub> concentrations is shown in **Figure I1.14**. All general ambient locations are in compliance with the respective proposed annual AQO. The highest concentration upon the implementation of Phase II control measures is 35 µg/m<sup>3</sup>, which is in compliance with the respective proposed new AQO value of 40 µg/m<sup>3</sup>.



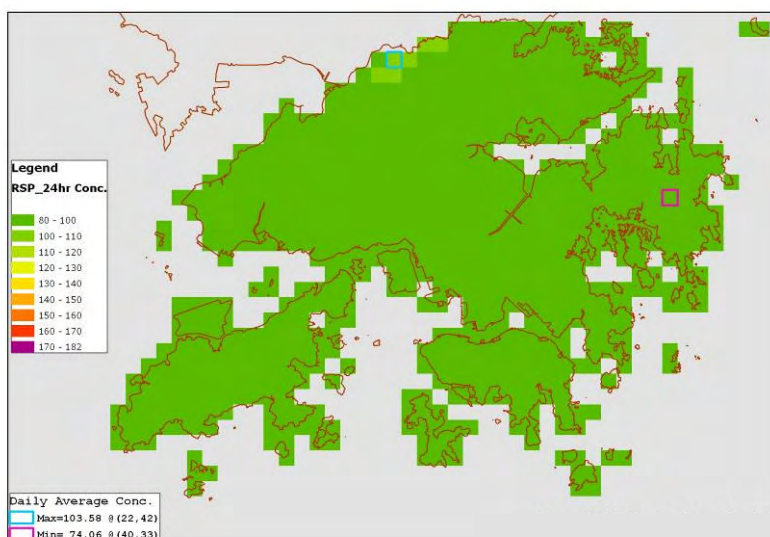
**Figure I1.14:** Spatial distribution of annual NO<sub>2</sub> concentration upon implementation of Phase II measures



### 11.2.3.3 Respirable Suspended Particulates (PM<sub>10</sub>)

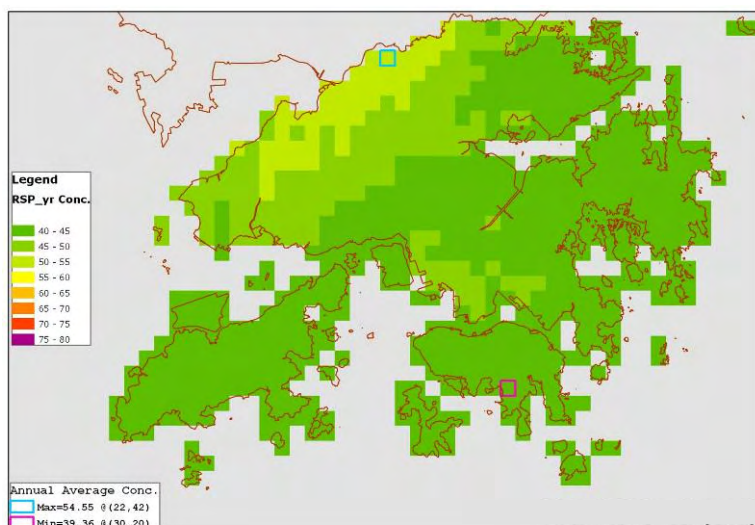
PATH model run has been conducted on 24-hr averaged and annual PM<sub>10</sub>. The spatial distribution of the 10<sup>th</sup> highest 24-hr averaged PM<sub>10</sub> concentration is shown in **Figure I1.15**. The highest figure upon implementation of the Phase II control measures is 104 µg/m<sup>3</sup>, which is marginally higher than the new AQO of 100 µg/m<sup>3</sup>. Owing to the susceptibility of being influenced by trans-boundary air pollution, the highest 24-hr averaged PM<sub>10</sub> concentration is observed at the boundary with Shenzhen. Other than the few spots at the area near the boundary, the highest figure is 100 µg/m<sup>3</sup>, which is in compliance with the respective proposed new AQO.

**Figure I1.15:** Spatial distribution of the 10<sup>th</sup> highest 24-hr averaged PM<sub>10</sub> concentration upon implementation of Phase II measures



Similar to the 24-hr averaged PM<sub>10</sub> concentration, the highest annual PM<sub>10</sub> concentration is observed at the boundary with Shenzhen. The predicted concentration is 55 µg/m<sup>3</sup>, which is marginally higher than the respective proposed new AQO of 50 µg/m<sup>3</sup>. The spatial distribution of the annual averaged PM<sub>10</sub> concentrations is shown in **Figure I1.16**.

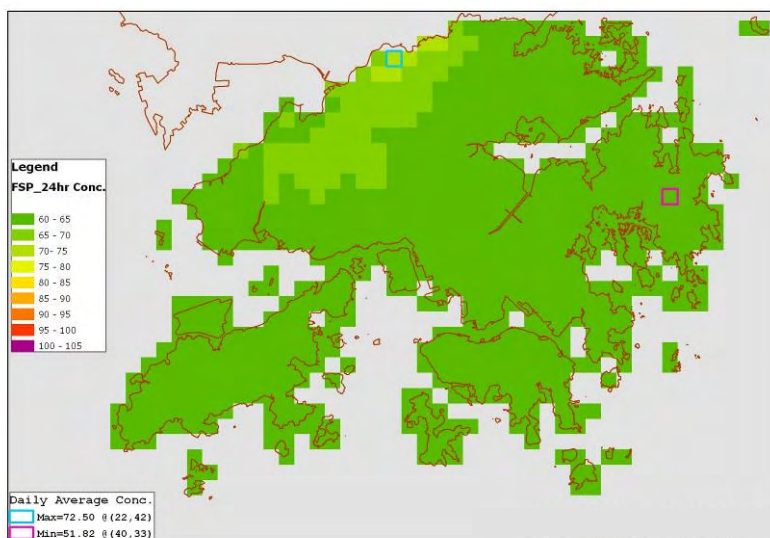
**Figure I1.16:** Spatial distribution of annual  $PM_{10}$  concentration upon implementation of Phase II measures



#### I1.2.3.4 Fine Suspended Particulates ( $PM_{2.5}$ )

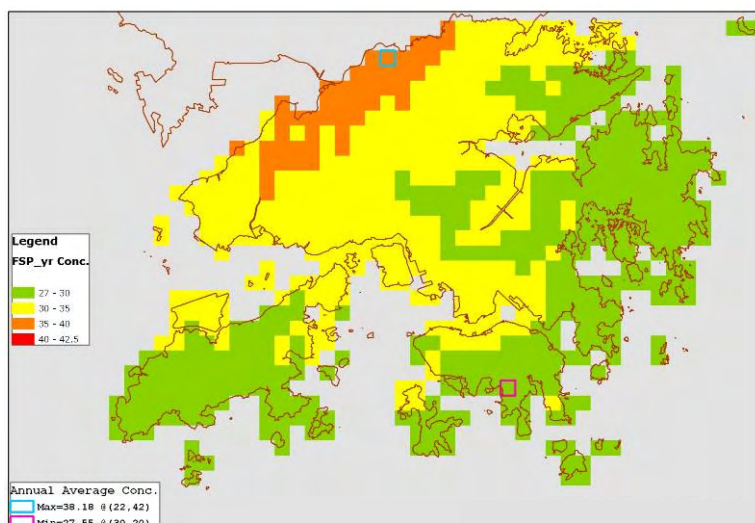
The  $PM_{2.5}$  levels were estimated by multiplying the average  $PM_{2.5}/PM_{10}$  ratio of 0.7 (derived from existing air quality monitoring stations) on the predicted  $PM_{10}$  value. The spatial distribution of the 10<sup>th</sup> highest 24-hr averaged  $PM_{2.5}$  concentration is shown in **Figure I1.17**. The highest figure upon implementation of Phase II control measures is estimated to be about  $73 \mu g/m^3$ , which is in compliance with the respective proposed new AQO.

**Figure I1.17:** Spatial distribution of 10<sup>th</sup> highest 24-hr averaged  $PM_{2.5}$  concentration upon implementation of Phase II measures



Similar to  $PM_{10}$ , the highest annual  $PM_{2.5}$  concentration occurs at the boundary with Shenzhen. Due to the likely contribution of the trans-boundary emissions, the annual  $PM_{2.5}$  concentration, upon implementation of Phase II control measures, is  $38 \mu g/m^3$ , which is marginally higher than the respective proposed new AQO value of  $35 \mu g/m^3$ . The spatial distribution of the annual averaged  $PM_{10}$  concentrations are shown in **Figure I1.18**.

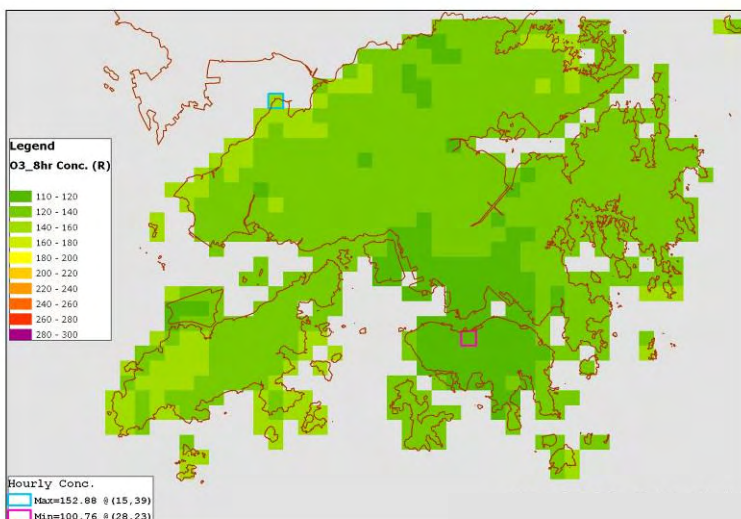
**Figure I1.18:** Spatial distribution of annual PM<sub>2.5</sub> concentration upon implementation of Phase II measures



#### I1.2.3.5 Ozone

PATH model run has been conducted for ozone. The spatial distribution of the 10<sup>th</sup> highest 8-hr averaged ozone concentrations is shown in **Figure I1.19**. The highest figure upon implementation of Phase II measures is 153  $\mu\text{g}/\text{m}^3$ , which is in compliance with the respective proposed new AQO.

**Figure I1.19:** Spatial distribution of 10<sup>th</sup> highest 8-hr averaged Ozone concentration upon implementation of Phase II measures



#### I1.2.3.6 Carbon Monoxide and Lead

PATH model run has not been conducted for carbon monoxide and lead as they have already been in compliance with the respective proposed new AQOs. It is expected that the compliance status will be maintained as the emissions would further be reduced upon the implementation of Phase II control measures.

### I1.2.4 Phase III Long Term Measures (Low Emission Scenario)

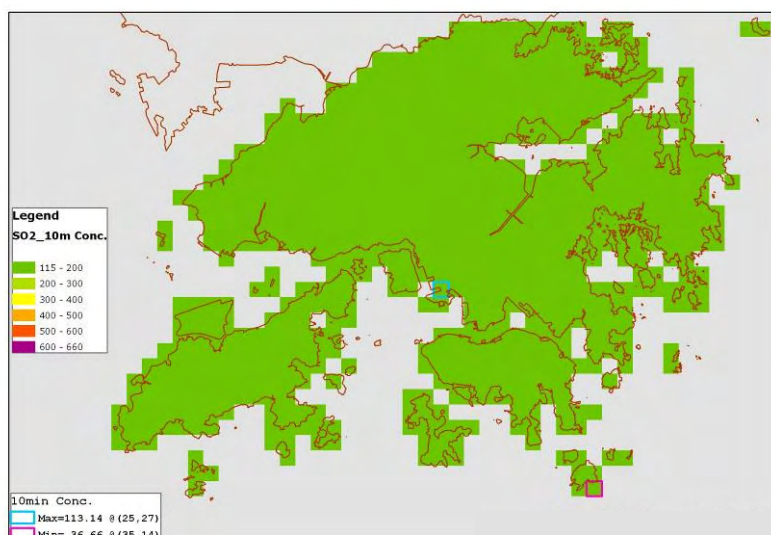
#### I1.2.4.1 Sulphur Dioxide

PATH model run has been conducted on SO<sub>2</sub>. As the PATH model does not have the algorithm for predicting concentrations with averaging time less than 1 hour, the 10min SO<sub>2</sub> concentrations are derived from the respective predicted 1-hr SO<sub>2</sub> levels (Please refer to section H1.2.2.1 for the relationship).



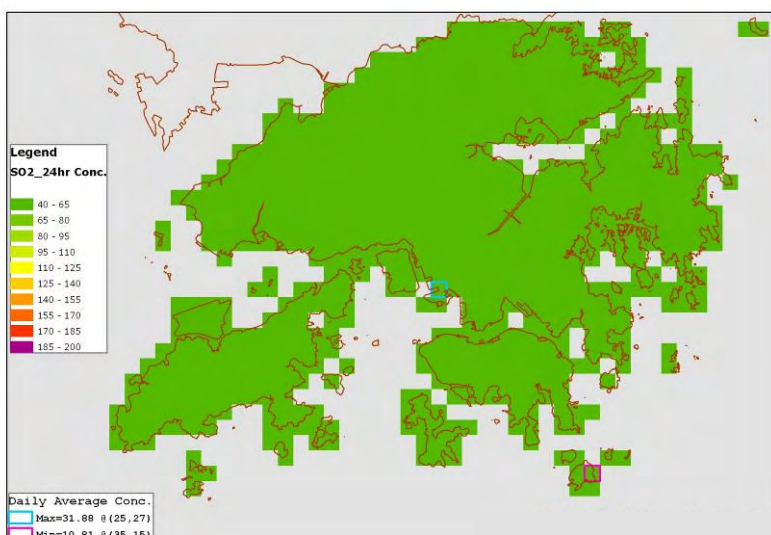
The spatial distribution of 4<sup>th</sup> highest 10-min SO<sub>2</sub> is shown in **Figure I1.20**. The highest figure upon the implementation of Phase III control measures is 113 µg/m<sup>3</sup>, which is in compliance with the respective proposed new AQO of 500 µg/m<sup>3</sup>.

**Figure I1.20:** Spatial distribution of 4<sup>th</sup> highest 10-min SO<sub>2</sub> concentration upon implementation of Phase III measures



The spatial distribution of 4<sup>th</sup> highest 24-hr averaged SO<sub>2</sub> is shown in **Figure I1.21**. The highest figure is 32 µg/m<sup>3</sup> which is in compliance with the respective proposed new AQO of 125 µg/m<sup>3</sup>.

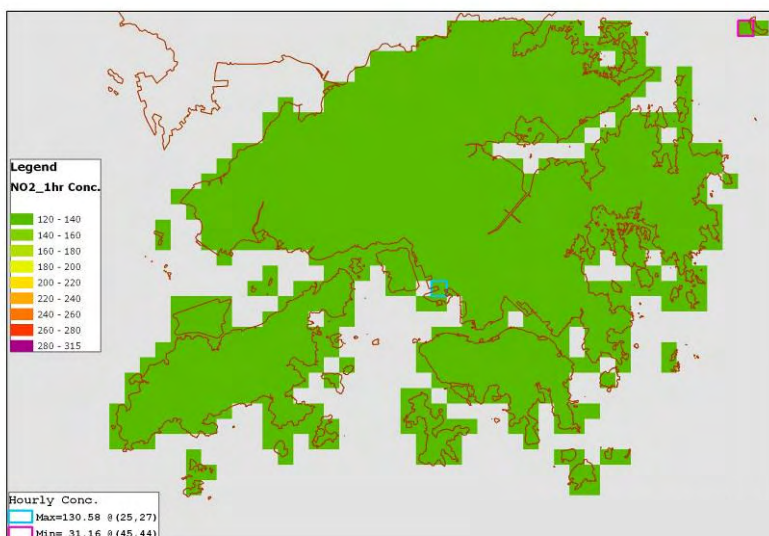
**Figure I1.21:** Spatial distribution of 4<sup>th</sup> highest 24-hr averaged SO<sub>2</sub> concentration upon implementation of Phase III measures



#### I1.2.4.2 Nitrogen Dioxide

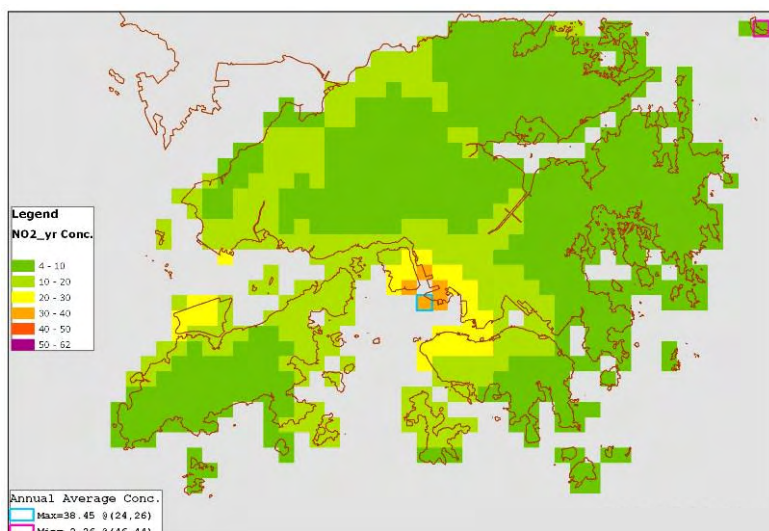
PATH model run has been conducted on 1-hr NO<sub>2</sub>. The spatial distribution of the 19<sup>th</sup> highest 1-hr NO<sub>2</sub> concentrations is shown in **Figure I1.22**. The highest figure upon the implementation of Phase III control measures is 131 µg/m<sup>3</sup>, which is in compliance with the respective proposed new AQO of 200 µg/m<sup>3</sup>.

**Figure I1.22:** Spatial distribution of 19<sup>th</sup> highest 1-hr NO<sub>2</sub> concentration upon implementation of Phase III measures



The spatial distribution of the annual NO<sub>2</sub> concentrations is shown in **Figure I1.23**. All general ambient locations are in compliance with the proposed annual AQO. The highest figures upon the implementation of Phase III control measures is 38.5  $\mu\text{g}/\text{m}^3$ , which is less than the respective proposed new AQO value of 40  $\mu\text{g}/\text{m}^3$ .

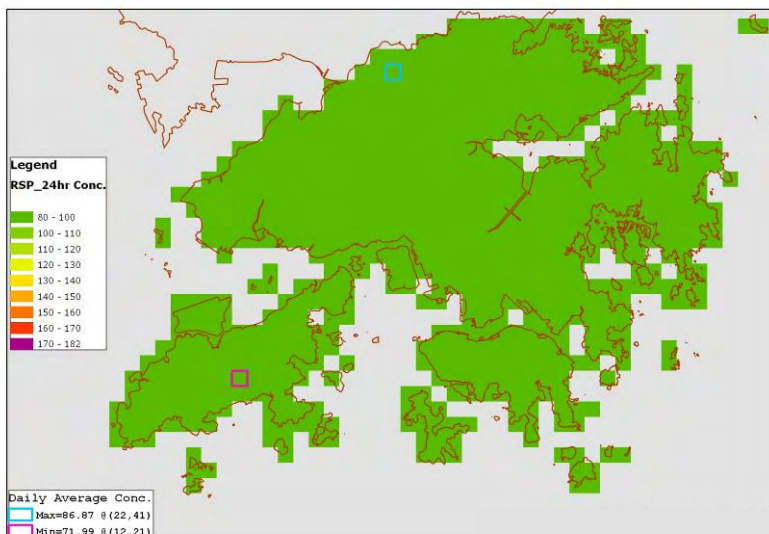
**Figure I1.23:** Spatial distribution of annual NO<sub>2</sub> concentration upon implementation of Phase III measures



#### I1.2.4.3 Respirable Suspended Particulates (PM<sub>10</sub>)

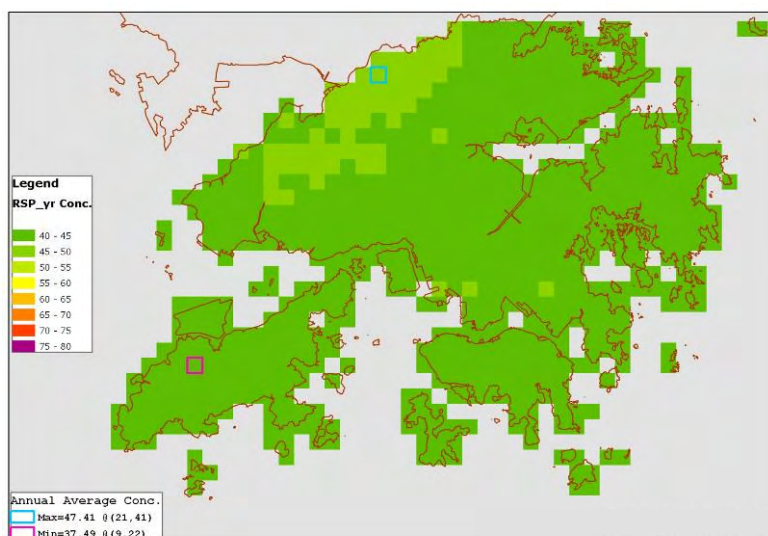
PATH model run has been conducted on 24-hr averaged and annual PM<sub>10</sub>. The spatial distribution of the 10<sup>th</sup> highest 24-hr averaged PM<sub>10</sub> concentration is shown in **Figure I1.24**. The highest figure upon implementation of the Phase III control measures is 87  $\mu\text{g}/\text{m}^3$ , which is in compliance with the respective proposed new AQO.

**Figure I1.24:** Spatial distribution of 10<sup>th</sup> highest 24-hr averaged PM<sub>10</sub> concentration upon implementation of Phase III measures



Similar to the 24-hr averaged PM<sub>10</sub> concentration, the highest annual PM<sub>10</sub> concentration is observed at the boundary with Shenzhen. The predicted concentration would be 47.4 µg/m<sup>3</sup>, which is in compliance with the respective proposed new AQO of 50 µg/m<sup>3</sup>. The spatial distribution of the annual averaged PM<sub>10</sub> concentrations are shown in **Figure I1.25**.

**Figure I1.25:** Spatial distribution of annual PM<sub>10</sub> concentration upon implementation of Phase III measures

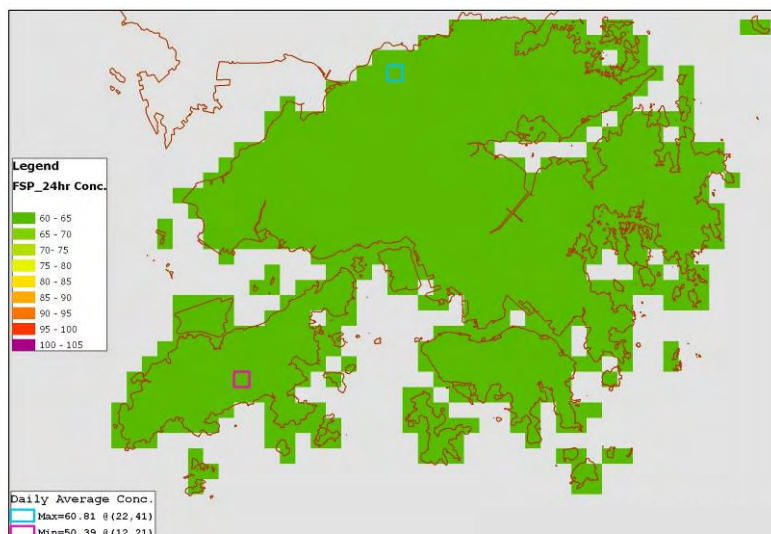


#### I1.2.4.4 Fine Suspended Particulates (PM<sub>2.5</sub>)

The PM<sub>2.5</sub> levels were estimated by multiplying the average PM<sub>2.5</sub>/PM<sub>10</sub> ratio of 0.7 (derived from existing air quality monitoring stations) on the predicted PM<sub>10</sub> value. The spatial distribution of the 10<sup>th</sup> 24-hr averaged PM<sub>2.5</sub> concentration is shown in **Figure I1.26**. The highest figure upon implementation of Phase III control measures is estimated to be about 61 µg/m<sup>3</sup>, which is in compliance with the respective proposed new AQO value of 75 µg/m<sup>3</sup>.

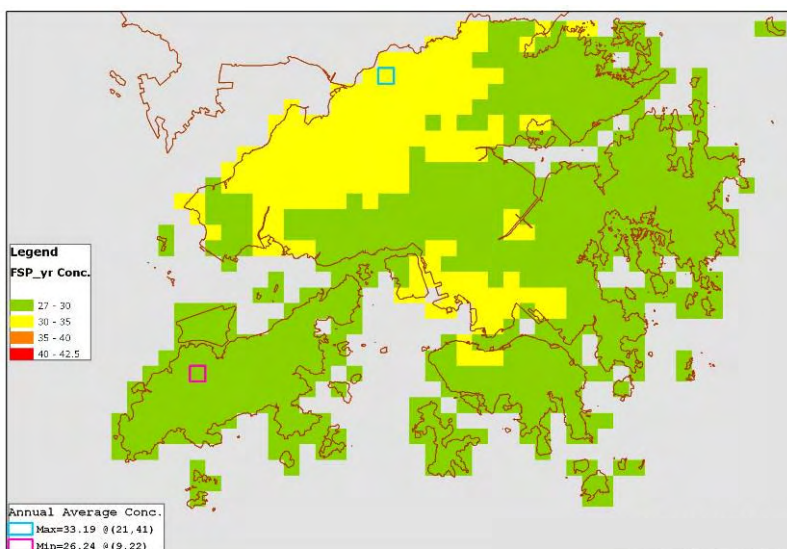


**Figure I1.26:** Spatial distribution of 10<sup>th</sup> highest 24-hr averaged PM<sub>2.5</sub> concentration upon implementation of Phase III measures



Similar to PM<sub>10</sub>, the highest annual PM<sub>2.5</sub> concentration occurs at the boundary with Shenzhen. Due to the likely contribution of the trans-boundary emissions, the annual PM<sub>2.5</sub> concentration, upon implementation of Phase III control measures, would be 33 µg/m<sup>3</sup>, which is in compliance with the respective proposed new AQO value of 35 µg/m<sup>3</sup>. The spatial distribution of the annual averaged PM<sub>10</sub> concentrations is shown in **Figure I1.27**.

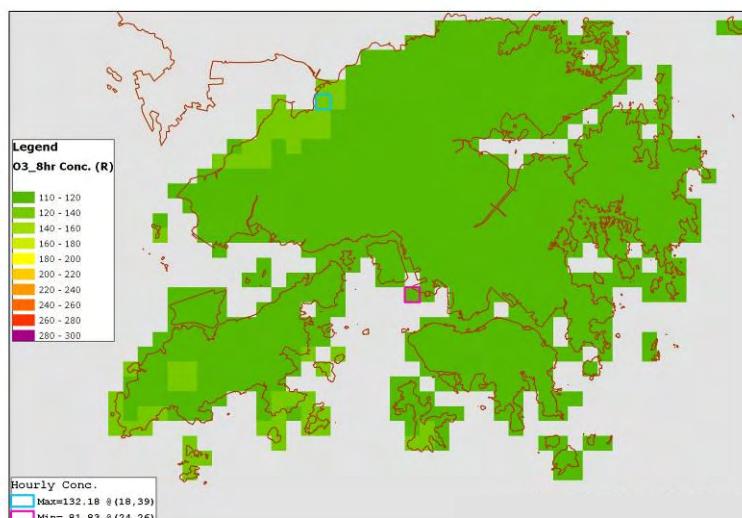
**Figure I1.27:** Spatial distribution of annual PM<sub>2.5</sub> concentration upon implementation of Phase III measures



#### I1.2.4.5 Ozone

PATH model run has been conducted for ozone. The spatial distribution of the 10<sup>th</sup> highest 8-hr averaged ozone concentrations is shown in **Figure I1.28**. The highest figure upon implementation of Phase III measures is 132 µg/m<sup>3</sup>, which is in compliance with the respective proposed new AQO.

**Figure I1.28:** Spatial distribution of 10<sup>th</sup> highest 8-hr averaged Ozone concentration upon implementation of Phase III measures



#### I1.2.4.6 Carbon Monoxide and Lead

PATH model run has not been conducted for carbon monoxide and lead as they have already been in compliance with the respective proposed new AQOs. It is expected that the compliance status will be maintained as the emissions would further be reduced upon the implementation of Phase III control measures.

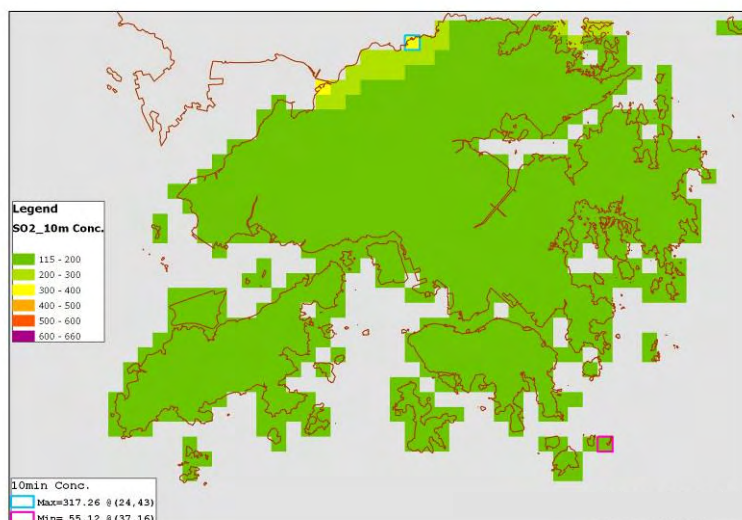
#### I1.2.5 Phase III Long Term Measures (High Emission Scenario)

##### I1.2.5.1 Sulphur Dioxide

PATH model run has been conducted on SO<sub>2</sub>. As the PATH model does not have the algorithm for predicting concentrations with averaging time less than 1 hour, the 10min SO<sub>2</sub> concentrations are derived from the respective predicted 1-hr SO<sub>2</sub> levels (Please refer to section H1.2.2.1 for the relationship).

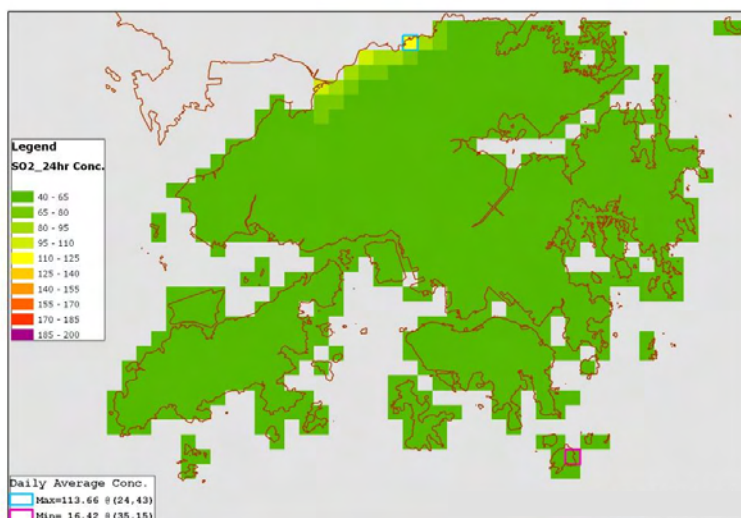
The spatial distribution of 4<sup>th</sup> highest 10-min SO<sub>2</sub> is shown in **Figure I1.29**. The highest figure upon the implementation of Phase III control measures is 317 µg/m<sup>3</sup>, which is in compliance with the respective proposed new AQO of 500 µg/m<sup>3</sup>.

**Figure I1.29:** Spatial distribution of 4<sup>th</sup> highest 10-min SO<sub>2</sub> concentration upon implementation of Phase III measures (High Emission Scenario)



The spatial distribution of 4<sup>th</sup> highest 24-hr averaged SO<sub>2</sub> is shown in **Figure I1.30**. The highest figure is 114 µg/m<sup>3</sup> which is in compliance with the respective proposed new AQO of 125 µg/m<sup>3</sup>.

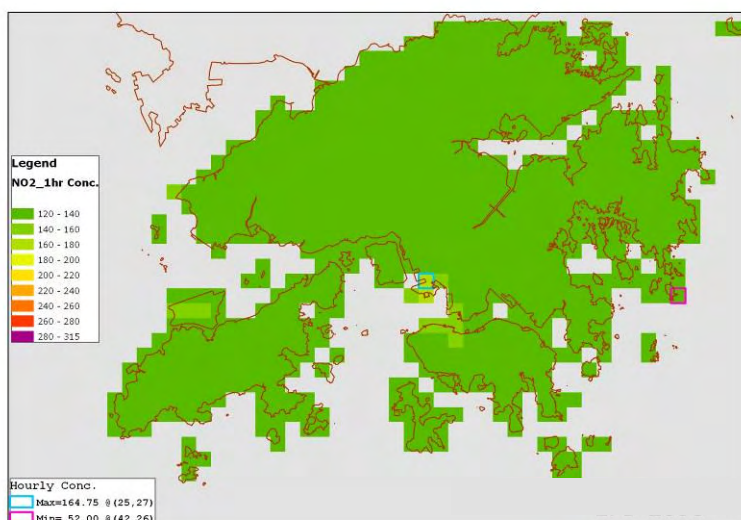
**Figure I1.30:** Spatial distribution of 4<sup>th</sup> highest 24-hr averaged SO<sub>2</sub> concentration upon implementation of Phase III measures (High Emission Scenario)



#### I1.2.5.2 Nitrogen Dioxide

PATH model run has been conducted on 1-hr NO<sub>2</sub>. The spatial distribution of the 19<sup>th</sup> highest 1-hr NO<sub>2</sub> concentrations is shown in **Figure I1.31**. The highest figure upon the implementation of Phase III control measures is 165 µg/m<sup>3</sup>, which is in compliance with the respective proposed new AQO of 200 µg/m<sup>3</sup>.

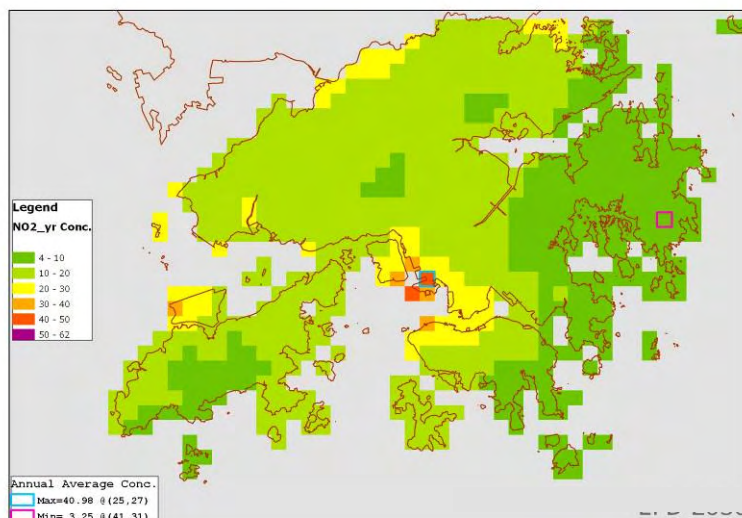
**Figure I1.31:** Spatial distribution of 19<sup>th</sup> highest 1-hr NO<sub>2</sub> concentration upon implementation of Phase III measures (High Emission Scenario)



The spatial distribution of the annual NO<sub>2</sub> concentrations is shown in **Figure I1.32**. Other than a few spots at the container terminal areas which are of less concern to the general public, all general ambient locations are in compliance with the respective proposed new AQO. Similar to practice of other countries such as UK, long term (i.e., annual) AQO will not be applicable to places of work where members of the public do not have regular access. The highest figure at other locations is 36 µg/m<sup>3</sup>, which is less than the respective proposed new AQO value of 40 µg/m<sup>3</sup>.



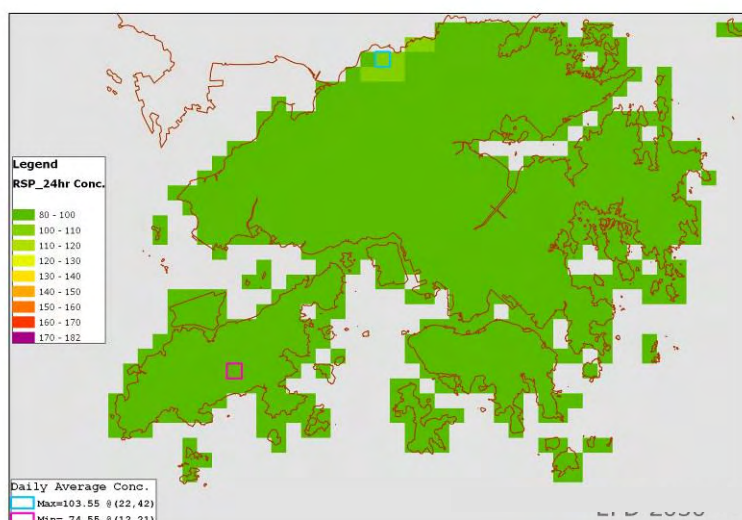
**Figure I1.32:** Spatial distribution of annual  $\text{NO}_2$  concentration upon implementation of Phase III measures (High Emission Scenario)



#### 11.2.5.3 Respirable Suspended Particulates ( $\text{PM}_{10}$ )

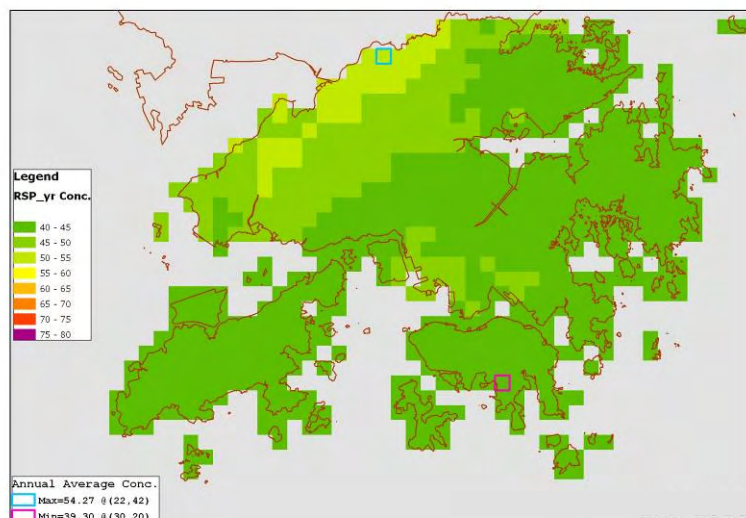
PATH model run has been conducted on 24-hr averaged and annual  $\text{PM}_{10}$ . The spatial distribution of the 10<sup>th</sup> highest 24-hr averaged  $\text{PM}_{10}$  concentration is shown in **Figure I1.33**. The highest figure upon implementation of the Phase III control measures is  $104 \mu\text{g}/\text{m}^3$ , which is marginally higher than the respective proposed new AQO. Owing to the susceptibility of being influenced by trans-boundary air pollution, the highest 24-hr averaged  $\text{PM}_{10}$  concentration is observed at the boundary with Shenzhen. Other than the few spots at the area near the boundary, the highest figure is  $100 \mu\text{g}/\text{m}^3$ , which is in compliance with the respective proposed new AQO.

**Figure I1.33:** Spatial distribution of 10<sup>th</sup> highest 24-hr averaged  $\text{PM}_{10}$  concentration upon implementation of Phase III measures (High Emission Scenario)



Similar to the 24-hr averaged  $\text{PM}_{10}$  concentration, the highest annual  $\text{PM}_{10}$  concentration is observed at the boundary with Shenzhen. The predicted concentration would be  $54 \mu\text{g}/\text{m}^3$ , which is marginally higher than the respective proposed new AQO of  $50 \mu\text{g}/\text{m}^3$ . The spatial distribution of the annual averaged  $\text{PM}_{10}$  concentrations are shown in **Figure I1.34**.

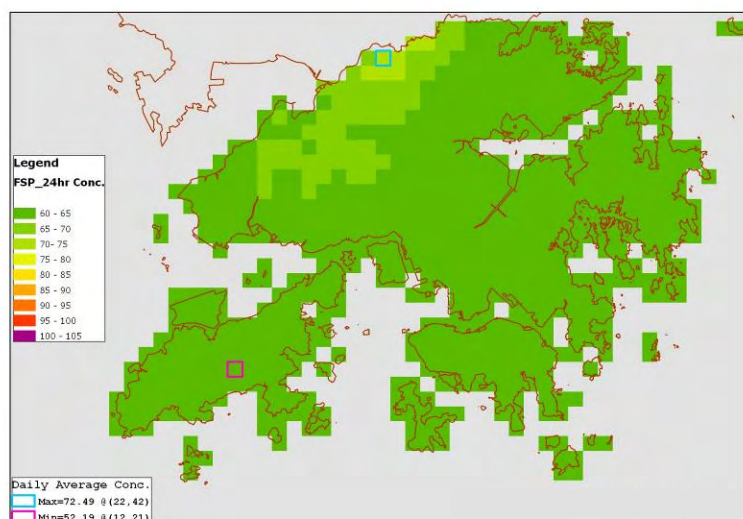
**Figure I1.34:** Spatial distribution of annual  $PM_{10}$  concentration upon implementation of Phase III measures (High Emission Scenario)



#### I1.2.5.4 Fine Suspended Particulates ( $PM_{2.5}$ )

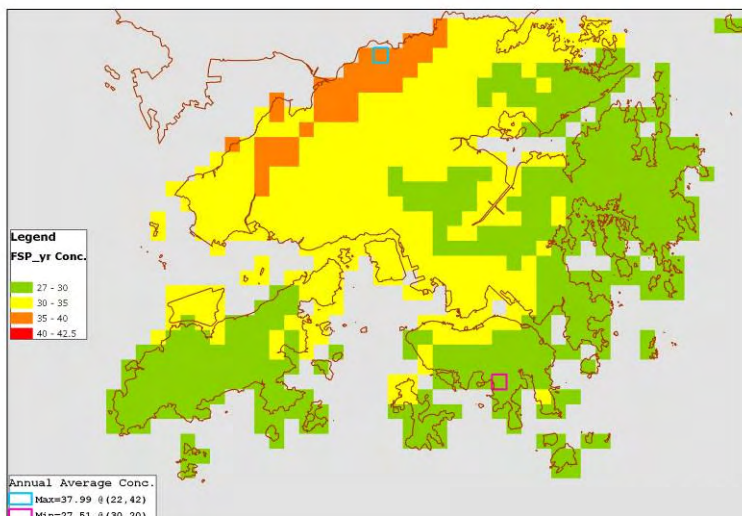
The  $PM_{2.5}$  levels were estimated by multiplying the average  $PM_{2.5}/PM_{10}$  ratio of 0.7 (derived from existing air quality monitoring stations) on the predicted  $PM_{10}$  value. The spatial distribution of the 10<sup>th</sup> 24-hr averaged  $PM_{2.5}$  concentration is shown in **Figure I1.35**. The highest figure upon implementation of Phase III control measures is estimated to be about  $72 \mu g/m^3$ , which is in compliance with the respective proposed new AQO value of  $75 \mu g/m^3$ .

**Figure I1.35:** Spatial distribution of 10<sup>th</sup> highest 24-hr averaged  $PM_{2.5}$  concentration upon implementation of Phase III measures (High Emission Scenario)



Similar to  $PM_{10}$ , the highest annual  $PM_{2.5}$  concentration occurs at the boundary with Shenzhen. Due to the likely contribution of the trans-boundary emissions, the annual  $PM_{2.5}$  concentration, upon implementation of Phase III control measures, would be  $38 \mu g/m^3$ , which is which is marginally higher than the respective proposed new AQO value of  $35 \mu g/m^3$ . The spatial distribution of the annual averaged  $PM_{10}$  concentrations is shown in **Figure I1.36**.

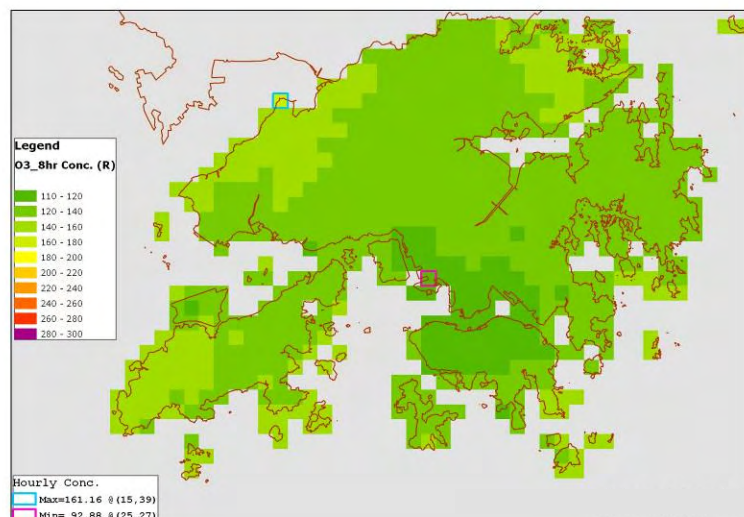
**Figure I1.36:** Spatial distribution of annual PM<sub>2.5</sub> concentration upon implementation of Phase III measures (High Emission Scenario)



#### 11.2.5.5 Ozone

PATH model run has been conducted for ozone. The spatial distribution of the 10<sup>th</sup> highest 8-hr averaged ozone concentrations is shown in **Figure I1.37**. The highest figure upon implementation of Phase III measures is observed at the remote area of Deep Day. The highest figure upon implementation of Phase III measures is 161 µg/m<sup>3</sup>, which is marginally higher than the respective proposed new AQO of 160 µg/m<sup>3</sup>. Other than the few spots at the area the remote area of Deep Day, the highest figure is 157 µg/m<sup>3</sup>, which is in compliance with the respective proposed new AQO.

**Figure I1.37:** Spatial distribution of 10<sup>th</sup> highest 8-hr averaged Ozone concentration upon implementation of Phase III measures (High Emission Scenario)



#### 11.2.5.6 Carbon Monoxide and Lead

PATH model run has not been conducted for carbon monoxide and lead as they have already been in compliance with the respective proposed new AQOs. It is expected that the compliance status will be maintained as the emissions would further be reduced upon the implementation of Phase III control measures.